

Electronic structure of the Si(001) surface with Pb adsorbates

Kensuke Tono

Department of Chemistry, The University of Tokyo, Hongo, Tokyo 113-0033, Japan

Han Woong Yeom*

Atomic-scale Surface Science Research Center and Institute of Physics and Applied Physics, Yonsei University, Seoul 120-790, Korea

Iwao Matsuda and Toshiaki Ohta

Department of Chemistry, The University of Tokyo, Hongo, Tokyo 113-0033, Japan

(Received 16 November 1999)

The electronic structures of the Pb-adsorbed Si(001) surface have been studied by angle-resolved photoelectron spectroscopy (ARPES) using synchrotron radiation. In addition to the evolution of surface electronic states during Pb initial growth at room temperature up to ~ 2 monolayers (ML's), detailed surface-state band dispersions were investigated for the single-domain 2×2 -Pb and 2×1 -Pb surfaces occurring at ~ 0.5 and ~ 1.0 ML, respectively. On the 2×2 -Pb surface, four surface-state bands were identified within the bulk band gap. The surface band structure of the 2×2 -Pb surface is close to that of the Si(001) 2×2 -Al (In) surface suggesting an overall similarity of their surface structures. While the 2×2 -Pb surface is found to be semiconducting with a band gap larger than 0.5 eV, the 2×1 -Pb surface is revealed to be metallic with five different surface-state bands. Above 1.0 ML, the ARPES spectra of the Pb/Si(001) surface hardly change with increasing the Pb coverage. The correlation between the surface electronic structures and the intriguing surface structures of different Pb coverages is discussed.

I. INTRODUCTION

The adsorption of group-IV elements on elemental semiconductor surfaces has been extensively studied due to its technological and fundamental importance. Especially the Ge and Si adsorption systems are treated as the model systems of hetero- and homoepitaxy on silicon, respectively.¹⁻⁴ On the other hand, the Pb/Si system has attracted interest as a typical metal/semiconductor interface due to the negligible mutual solubility of Pb and Si. Although most of the previous studies on the Pb/Si surfaces have concentrated on the Si(111) substrate,⁵ the recent scanning tunneling microscopy (STM) studies unveiled the unique and interesting features of the initial Pb growth on the Si(001) surface.^{6,7}

For instance, the well-defined single-atom-wide chains of Pb adsorbates were identified for the Pb coverage less than 0.5 monolayers (ML's) at room temperature.^{6,8} This one-dimensional (1D) feature resembles the well-established parallel-dimer chains of Al, Ga, and In adsorbates on the Si(001) surface, which are composed of symmetric addimers in parallel to the chains and to the substrate Si dimers [see Fig. 1(a)].⁹⁻¹⁶ However, the Pb chains are reported to consist of *buckled parallel dimers* [Fig. 1(b)].⁶ The same buckled-parallel-dimer model has also been applied for the closely related systems of the Sn/Si(001) and Pb/Ge(001) surfaces.¹⁷⁻¹⁹ Similar parallel-dimer chains are also observed as metastable species for the Ge and Si initial growth on the Si(001) 2×1 surface but the buckling of dimers has not been discussed.²⁰⁻²² The recent *ab initio* total-energy calculations supported the buckled-parallel dimer configuration for the Pb/Si(001) and Pb/Ge(001) surfaces.^{23,24} However, there has been no detailed structural analysis to confirm this unique structure model and, moreover, no detailed surface electronic

structure study is available yet in contrast to the group-III adsorbate systems.^{14,16,25}

Another interesting feature of the Pb/Si(001) surface is its initial growth behavior beyond 0.5 ML. While the 2D growth of group-III adsorbates saturates at 0.5 ML with the highly packed parallel-dimer chains in a 2×2 lattice,^{26,27} the Pb 2D layer was reported to evolve further to form a $c(4 \times 8)$ phase at ~ 0.8 ML and a 2×1 phase at ~ 1 ML.^{6,7,28} It was even reported that the second and the third layers of Pb grow in a layer-by-layer fashion.²⁸ The complex surface structures of these Pb layers are uncertain. In particular, the 1-ML 2×1 structure was reported to have Pb dimers rotated by 90° compared to the conventional 1×2 phases formed by Ge and Si monolayers on Si(001). That is, the Pb monolayer is not in the conventional crystallographical stacking of a diamond structure. To our knowledge, two different structural models for the 2×1 -Pb phase have been proposed as shown in Figs. 1(c) and (d),^{6,29} but the validity of these models has not been examined satisfactorily so far.

In this paper, we report on a detailed angle-resolved photoelectron spectroscopy (ARPES) study for the Pb overlayers on the Si(001) 2×1 surface. The evolution of surface electronic structures are investigated for the Pb coverages up to ~ 2 ML's in the layer-by-layer growth regime at room temperature. Especially the detailed surface-state band dispersions are measured for the well ordered single-domain 2×2 and 2×1 surfaces at 0.5 and 1.0 ML, respectively. These results are discussed in terms of the proposed structure models of the 2×2 and 2×1 phases.

II. EXPERIMENT

The ARPES experiment using synchrotron radiation was performed at the vacuum ultraviolet beam line BL-7B of

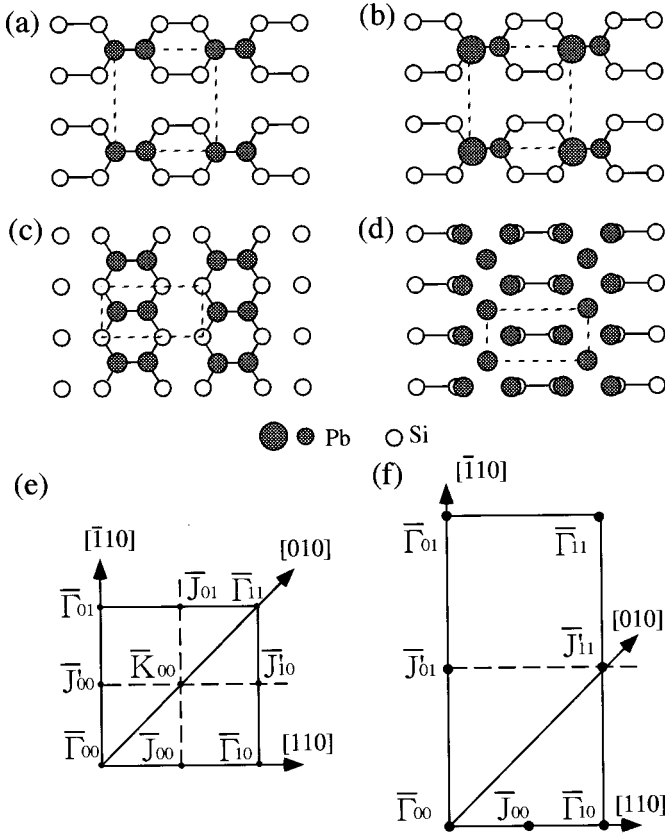


FIG. 1. Structural models for (a) the Si(001) 2×2 -Al (-Ga and -In) surface, (b) the Si(001) 2×2 -Pb surface (Ref. 6), and (c) and (d) for the Si(001) 2×1 -Pb surface proposed by STM (Ref. 1) and surface x-ray diffraction (Ref. 29), respectively. The surface unit cells are indicated by dashed rectangles. The (e) 2×2 and (f) 2×1 surface Brillouin zones with symmetry points marked.

Photon Factory, Japan. The details of ARPES apparatus has been reported before.³⁰ The overall angular and energy resolution chosen was $\sim 1.5^\circ$ and ~ 150 meV, respectively, at photon energies ($h\nu$) of 16.2 and 22.0 eV. The base pressure of the measurement chamber was under 2×10^{-10} mbars. For ARPES measurements, the incidence angle of photon with respect to the surface normal (θ_i) was fixed at 45° . At first, ARPES spectra for various Pb coverages were taken at two emission angles (θ_e) of 0 and 33° along the $[010]$ azimuth in order to monitor the evolution of surface states. For the well-ordered 2×2 -Pb and 2×1 -Pb surfaces, detailed angle-scan ARPES spectra were measured with an angular step of 2 or 3° along the major symmetric axes of the 2×2 and 2×1 surface Brillouin zones (SBZ's) [Figs. 1(e) and (f), respectively]. The Fermi level position (E_F) was determined from a cleaned Ta foil in direct contact with the Si substrate.

Using a mirror-polished and well-oriented Si(001) wafer (n type) as a substrate, a single-domain (SD) Si(001) 2×1 surface was prepared with a large terrace width as reported before.^{30,31} Pb was deposited onto the SD Si(001) 2×1 surface from a well-degassed Knudsen cell at a rate of ~ 0.13 ML/min. The pressure and substrate temperature during Pb deposition were held below 1×10^{-9} mbars and below 50°C , respectively. The clear SD 2×2 , SD 2×1 , and $c(4 \times 4)$ low-energy electron diffraction (LEED) patterns were observed at the Pb coverages of 0.4–0.6 ML, 1.0–2.0 ML, and above

2.0 ML's, respectively. Such evolution of LEED patterns with coverage is consistent with those reported previously²⁸ although we could not observe any clear $c(4 \times 8)$ LEED pattern reported in the range of 0.6–0.9 ML.

III. RESULTS AND DISCUSSION

A. Coverage dependent ARPES spectra

Figure 2 shows ARPES spectra at different Pb coverages taken with $h\nu = 16.2$ eV at θ_e of (a) 0° (normal emission) and (b) 33° along the $[010]$ azimuth. This azimuth is taken because the bulk band gap at off-normal emission angles is much wider than other azimuth making the identification of a surface state easier. The spectral feature denoted as **b** in Fig. 3(b) is due to the well-known bulk direct transition.³² The energy shift of **b** in the figure indicates the band bending induced by Pb adsorption. In particular, the binding energy (E_B) of **b** for the 2×2 -Pb (at 0.5 ML) and 2×1 -Pb (at 1.0 ML) surfaces shifts toward the lower energy by ~ 0.15 and ~ 0.1 eV from that of the clean surface, respectively. The prominent peak at $E_B \sim 0.6$ eV in Fig. 2(a) (denoted as **A**) on the clean surface spectrum is the well-known dangling-bond surface state of the Si(001) 2×1 surface.^{32,33} This dangling-bond state splits into two spectral features at $\theta_e = 33^\circ$ [**A** and **B** in Fig. 2(b)].^{32,33} Upon increasing the Pb coverage, **A** and **B** show a gradual but conspicuous decrease in their intensities with increasing the Pb coverage. At ~ 0.5 ML, these two states are replaced by a different surface state S_1 with a much weaker intensity. In fact, from the spectra shown in Fig. 2, S_1 is not so easily identified from **A**. However, the detailed ARPES data given below indicate clearly that this state has different dispersion from that of **A**, which is consistent with the 2×2 surface periodicity observed by LEED. This confirms that S_1 is a different Pb-derived surface state intrinsic to the 2×2 surface phase. Other spectral features characteristic of the 2×2 -Pb surface at 0.5 ML are found at $E_B \sim 1.2$, ~ 2.0 , and ~ 3.5 eV, which are denoted as S_2 , S_3 , and S_4 , respectively. These states will be discussed further below.

While the change of spectra is gradual and rather continuous up to 0.5 ML, the change between 0.5 and 0.7 ML is very drastic along with the disappearance of the 2×2 LEED pattern. That is, S_2 , S_3 , and S_4 (and also other minor features) disappear and features SS_2 and SS_4 (E_B of ~ 1.6 and ~ 4.2 eV, respectively) emerge at both emission angles. One can also find a tiny but noticeable feature S at $\theta_e = 33^\circ$, which appears only at the coverage of ~ 0.7 ML. The behavior of S_1 looks different from S_2 , S_3 , and S_4 since it seems only to shift in binding energy. Between 0.7 and 1.0 ML, the intensity of SS_2 and SS_4 states gradually increase but that of S_1 decreases gradually. In addition, a nontrivial photoemission intensity is observed at E_F (marked with M in Fig. 2). This metallic state appears from ~ 0.7 ML and is obvious above 1.0 ML. More detailed discussion on the metallic character of the surface is made below together with the SS_2 and SS_4 states in relation to the 2×1 -Pb surface phase.

It is noteworthy that no noticeable change of the ARPES spectra has been observed above 1.0 ML. The 2×1 LEED pattern observable from ~ 1.0 ML also does not change at 1.0–2.0 ML. This suggests that no remarkable change of the

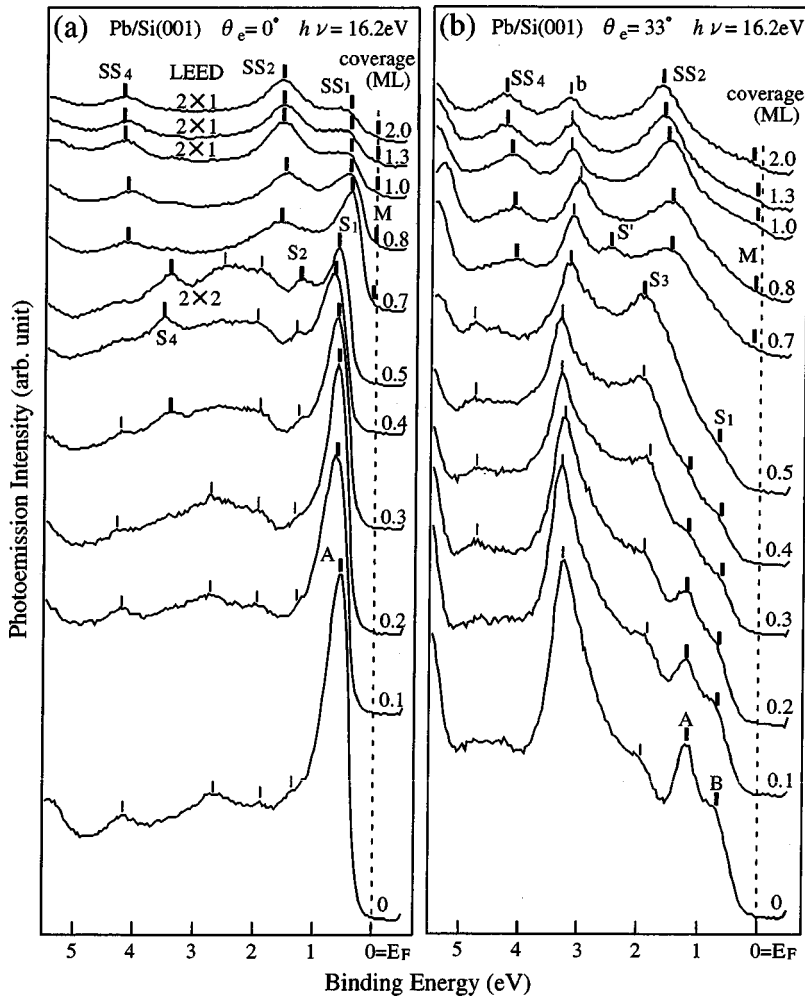


FIG. 2. ARPES spectra at different Pb coverages taken with a photon energy ($h\nu$) of 16.2 eV at emission angles (θ_e) of (a) 0° (normal emission) and (b) 33° along the $[010]$ azimuth. The incidence angle of photon (θ_i) is 45° . The LEED patterns observed for corresponding Pb coverages are indicated. The surface states assigned (see text for explanation) are marked with thick vertical bars.

surface structure occurs in spite of the growth of the second and third layers shown by STM. That is, the 2D layers above 1 ML seems not to destroy the registry of the 2×1 -Pb layer significantly and have a similar local structures as the 2×1 -Pb layer. In consistent with this suggestion, a recent STM study reported that the second Pb layer growing on the 2×1 -Pb surface also exhibits a 2×1 reconstruction with the same local dimer structure as that of the first layer.⁶ In contrast, another recent STM study reported a $c(4\times 4)$ reconstruction with symmetric Pb dimers of 0.25 ML on top of the asymmetric Pb dimer layer of 1 ML. This $c(4\times 4)$ phase is not consistent to the previous²⁸ and the present LEED observation although one cannot rule out the possibility of the existence of a locally ordered $c(4\times 4)$ phases at 1.25 ML.

B. Surface band structure of the 2×2 -Pb phase at half a monolayer

Detailed ARPES spectra for the 2×2 -Pb surface taken along the $[010]$ azimuth are shown in Fig. 3. The bulk-direct-transition feature **b** is observed at $21 < \theta_e < 48^\circ$. As the bulk band **b** is known to be located near the edge of the bulk band,³² the lower E_B region than **b** roughly corresponds to the bulk band gap. Within this band gap, two bands at $E_B \sim 0.6$ and ~ 1.9 eV are easily identified with little dispersions. These states correspond to S_1 and S_3 , respectively, mentioned above. S_1 appears as a dominant structure at $0 < \theta_e < 15^\circ$ but loses its intensity at larger θ_e . S_3 has a rela-

tively broad peak width. In a limited θ_e range of $0\sim 9^\circ$ or $18\sim 24^\circ$, a small features denoted as S_2 can be identified at $E_B \sim 1$ eV. Inside of the bulk bands region of $E_B \sim 3.5$ eV, another band, S_4 mentioned above, is observed. Although there are other minor spectral features, we concentrate mostly on the unambiguous surface states within the bulk band gap induced by Pb adsorption.

Figure 4 shows the dispersions of the spectral features observed on the 2×2 -Pb surface along the $[010]$ azimuth and also along the other two azimuths $[110]$ and $[\bar{1}10]$ (raw spectra not shown). In the figure, solid circles denote data points taken with $h\nu = 16.2$ eV and triangles with 22.0 eV. The three observed bands $S_1\sim S_3$ are within the bulk band gap indicating that they are the surface states. The invariance of their dispersions between the photon energies of 16.2 and 22.0 eV confirms the surface-state nature of $S_1\sim S_3$. $S_1\sim S_3$ show only little dispersions but it is clear that their dispersions follows the 2×2 SBZ symmetry. Hence, $S_1\sim S_3$ are thought to be intrinsic to the 2×2 -Pb surface phase. The coverage dependent ARPES data shown above suggested that S_4 (within the bulk band region) can also be due to a surface states of the 2×2 -Pb phase but no further evidence is obtained.

In order to assign the origin of the surface states observed, the detailed local structure of the 2×2 -Pb surface should be discussed. The present structure model of the 2×2 -Pb surface is composed of the 1D chains of parallel Pb dimers,

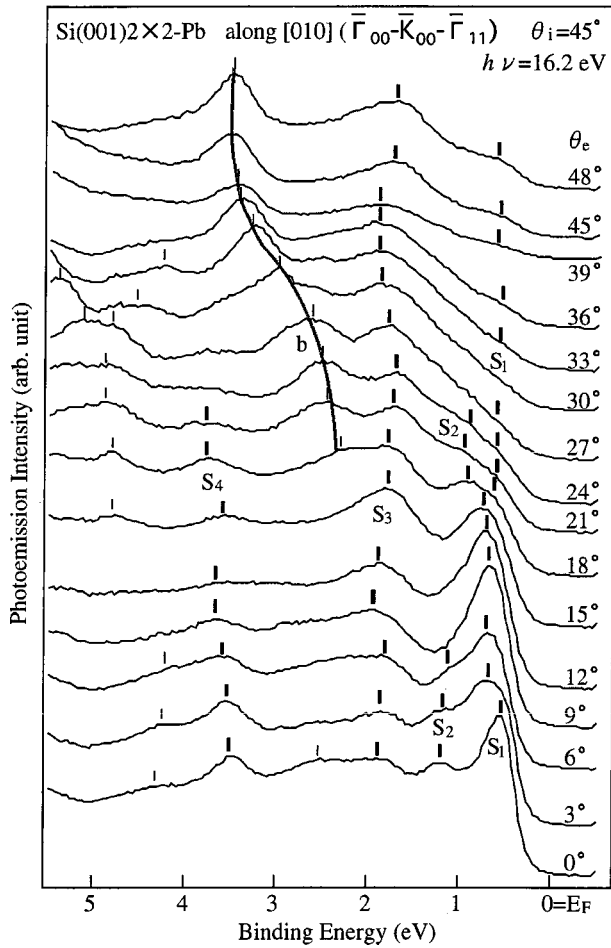


FIG. 3. Angle-scan ARPES spectra for the single-domain (SD) Si(001) 2×2 -Pb surface taken along the [010] azimuth (see Fig. 1) at $h\nu = 16.2$ eV. The incidence angle of photon (θ_i) is 45° . The emission angles (θ_e) are indicated for each spectrum which is normalized by the background intensity above the Fermi level (E_F). The surface states assigned (see text for explanation) are marked with thick vertical bars.

which is very close to the well-established 2×2 structures of the Al, Ga, and In adsorbates on the Si(001) surface except for the buckling of the dimers (see Fig. 1).¹²⁻¹⁶ For the symmetric parallel dimer structures of the 2×2 -Al, -Ga, and -In surfaces, the surface band structures have well been established:^{14,16,25,34} the surface bands are essentially identical with five surface states localized on the adsorbate dimers, i.e., the four back-bond (adsorbate-Si bond) and one dimer-bond (adsorbate-adsorbate bond) surface states.^{14,16,25} In Fig. 5, we directly compare the surface electronic structure of the 2×2 -Pb surface with that of the 2×2 -Al surface reported previously.^{14,25} The lowest binding energy surface states of 2×2 -Al is the dimer-bond state and the others the back-bond states. Two of the back-bond states depicted with lighter gray lines are odd symmetry states, which cannot easily be detected in the present measurement geometry. In this comparison, one can find the remarkable similarity between the band structures of the 2×2 -Pb and the 2×2 -Al surfaces. This obviously indicates the surface structures of these two surfaces are very close and thus the parallel dimer model is very plausible also for the 2×2 -Pb surface. Along this line of logic, it is tempting to assign S_1 as the Pb-Pb dimer-bond

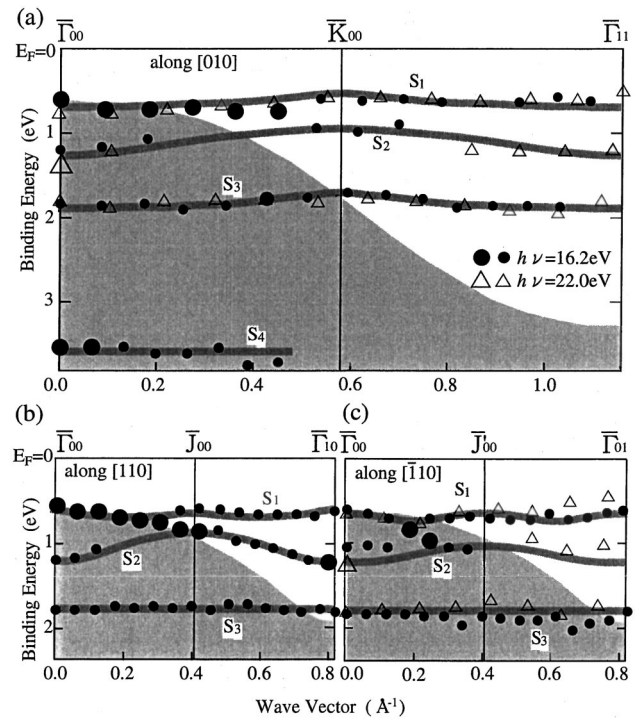


FIG. 4. Experimental dispersion curves for the surface states of SD Si(001) 2×2 -Pb surface along the (a) [010], (b) [110], and (c) $[\bar{1}10]$ axes. The solid circles and open triangles represent the data points taken with $h\nu = 16.2$ and 22.0 eV, respectively. The large and small symbols represent the relatively strong and weak spectral features, respectively. The hatched area shows the bulk bands projected onto the 1×1 SBZ. The thick gray lines are drawn to guide the dispersions determined.

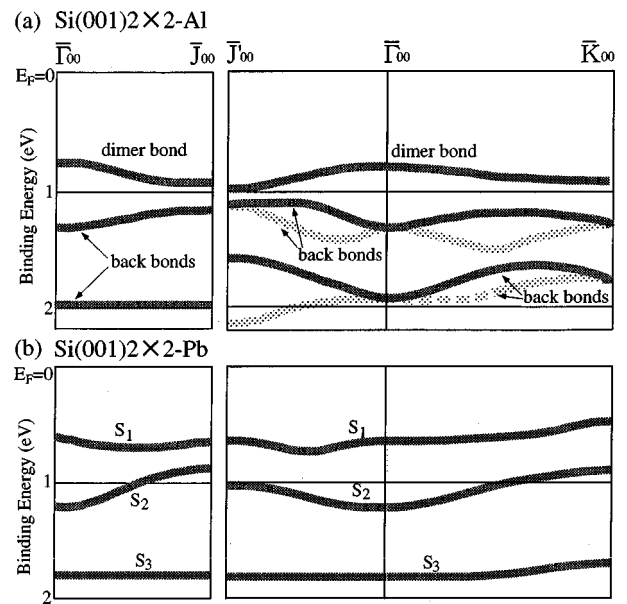


FIG. 5. Comparison of the dispersions of the surface states for (a) the Si(001) 2×2 -Al surface (Ref. 16) and (b) the Si(001) 2×2 -Pb surface. The origins of the surface states of the Si(001) 2×2 -Al surface are given as assigned in Ref. 16. Parts of the dispersions drawn with lighter gray lines are the odd-symmetry surface states, which cannot easily be detected in the present measurements for the Si(001) 2×2 -Pb surface (Ref. 16).

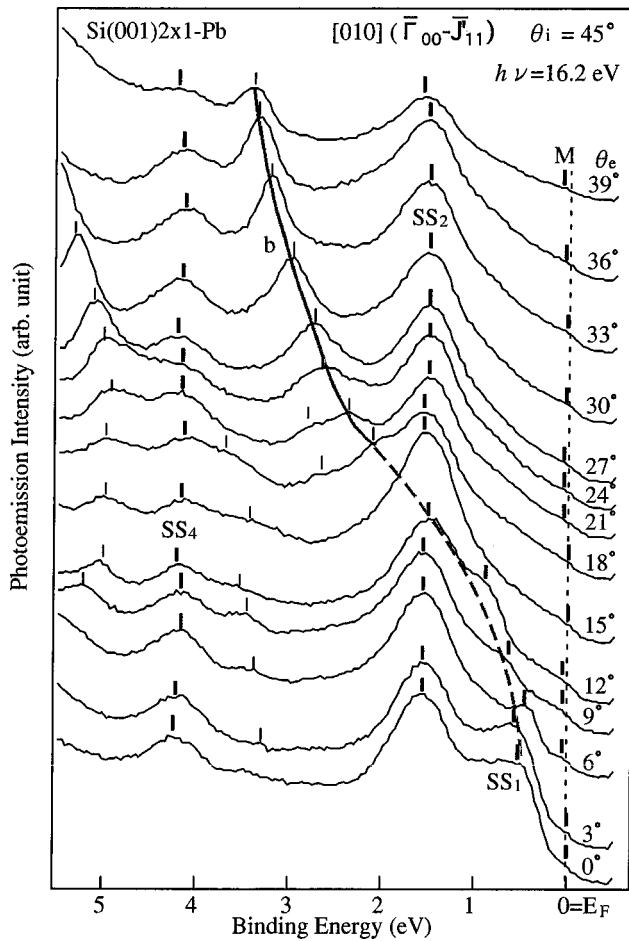


FIG. 6. Similar to the ARPES spectra of Fig. 3 but for the single-domain Si(001) 2×1 -Pb surface.

state and S_2 and S_3 as the Pb-Si back-bond states. This comparison however does not count the possibility of the buckling of the Pb dimers and the presence of an additional electronic state, the dangling-bond surface state of Pb dimers. With this simplification and with no available theoretical information on the electronic structure of the Pb asymmetric parallel dimers, the above assignment is only tentative at present.

It can also be noted that the surface band structure does not possess any noticeable anisotropy, i.e., any 1D character along the Pb chains, in contrast to the strongly anisotropic initial growth behavior forming the well-defined 1D adsorbate chains.⁹ This can be due to the formation of strong local covalent bonding within the Pb dimers and between Pb and Si surface atoms preventing the delocalization of surface electronic states along the 1D Pb chains. This behavior is also similar to the case of 1D chains induced by group-III elements on Si(001).^{14–16,25}

C. Surface band structure of the 2×1 -Pb phase at one monolayer

Figure 6 shows a series of ARPES spectra for the SD Si(001) 2×1 -Pb surface taken along the [010] azimuth. The dispersions of the observed bands are summarized in Fig. 7 for the [010] azimuth and also for the $[\bar{1}10]$ azimuth (raw spectra not shown). As mentioned in Sec. III A, three char-

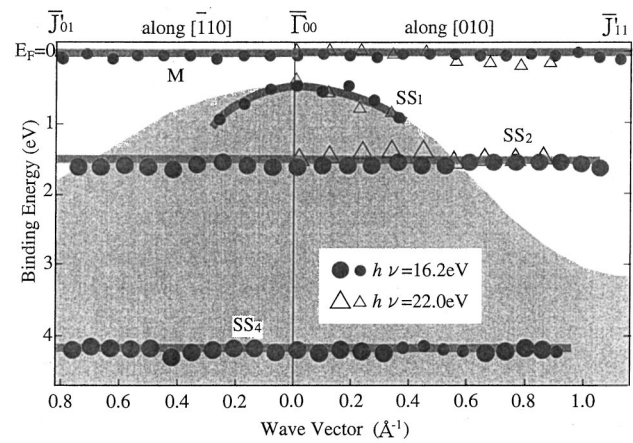


FIG. 7. Similar experimental dispersion curves to Fig. 4 but for the single-domain Si(001) 2×1 -Pb surface along the [010] and $[\bar{1}10]$ axes.

acteristic spectral features, M , SS_2 and SS_4 , are observed at E_F , 1.5 eV, and 4.2 eV, respectively. These three states commonly show no noticeable dispersions. The M and SS_2 states lie well within the bulk band gap and their dispersions are independent of the photon energy. This clearly indicates that M and SS_2 are the surface states. The coverage dependent spectra shown in Fig. 2 indicate that the appearance of M , SS_2 , and SS_4 is well correlated with the 2×1 LEED pattern. Thus we assign all these three states as the intrinsic surface states of the 2×1 -Pb phase at 1 ML. In clear contrast to the semiconducting 2×2 -Pb surface, the 2×1 -Pb surface is metallic due to the presence of M at E_F . In addition, a small spectral feature denoted as SS_1 can be found only around the normal emission at $E_B = 0.5 \sim 0.7$ eV. As shown in Fig. 7, SS_1 disperses following the edge of the bulk valence band suggesting that it might be the low binding energy part of the bulk band **b** (see the dashed gray line of Fig. 6). At $h\nu = 22.0$ eV, we observed another weak band SS_3 at $E_B \sim 2.0$ eV along the [010] azimuth within the band gap (Fig. 7).

Two different structure models of the 2×1 -Pb surface have been proposed so far. The model proposed by Itoh *et al.* is shown in Fig. 1(c), which consists of 1-ML symmetric Pb dimers.⁶ In this model the Si dimers seem to be preserved and the Pb dimers are parallel to the Si dimers. In contrast, another structural model has been mentioned, where two different Pb sites exist with a total coverage of 1.5 ML [see Fig. 1(d)]. However, this 1.5-ML model for the 2×1 surface does not agree with recent STM studies reporting the saturation of the first 2×1 layer at 1.0 ML.⁶ Our own coverage calibration by thickness monitor also indicates that the 2×1 phase is formed at $>1.0 \pm 0.15$ ML. Further, the characteristic spectral features of the 2×1 phase in ARPES spectra appears as early as 0.7 ML and then saturates at ~ 1.0 ML. Since the STM study also showed that the second layer on top of the first 2×1 layer also have a 2×1 registry,⁶ the 1.5-ML model may be related to a higher coverage phase than the first 2D layer. Based on this 1.5-ML structure model, Odasso *et al.* interpreted their ARPES results,²⁹ which observed two surface states (denoted as S and E) at E_B of ~ 0.5 and ~ 1.5 eV. They proposed that the S state is related to the dangling-bond state of the Si dimers of the clean surface and E to the Pb-Si bonds. However, it seems impossible that the bare Si dangling bonds are left even after

the saturation of the 1-ML 2D 2×1 -Pb layers as shown in STM.^{6,7} The Si dangling bonds must be saturated already on the 2×2 -Pb phase of 0.5 ML. The $S(E)$ state of the previous experiments is similar to SS_1 (SS_2) of the present study. After all, there are no reliable structural model and no theoretical calculations at present, which prevent any further discussion of the electronic structure of the 2×1 -Pb surface. However, the detailed surface-state dispersions given here will provide a crucial test of the structure models if a proper theoretical calculation is provided. It can be mentioned that the coverage-dependent ARPES data shown in Fig. 2 suggest a drastic change of the surface local structure between 0.5 and 0.7 ML. Thus a significantly different structure from the parallel dimers may be expected for the 2×1 -Pb surface.

Since the number of valence electrons in the 2×1 structure with 1 ML (or even with 1.5 ML) Pb is even, the surface should be semiconducting within the simple electron counting. However, the 2×1 -Pb surface is shown to be metallic with a substantial photoemission intensity at E_F . The previous photoemission study on the Pb/Si(001) surface³⁵ also reported an increase of photoemission intensity at E_F above 1 ML, which was then correlated with the presence of 3 D Pb islands. However, since the metallization start even from ~ 0.7 ML and the recent STM studies commonly observe no 3D islands up to 2 ML, we conclude that the metallic character is an inherent property of the Pb 2D layer. Assuming that the 2×1 -Pb surface consists of symmetric dimers as proposed by the STM studies, the surface metallicity might be due to the Pb dangling bond state of the symmetric dimers as in the case of the symmetric dimers of the Si(001) 2×1 surface.

IV. SUMMARY

The electronic structures of the Pb/Si(001) surface have been investigated by ARPES using synchrotron radiation.

This surface is shown to be semiconducting up to a Pb coverage of 0.5 ML and metallic above ~ 1.0 ML. On the single-domain Si(001) 2×2 -Pb surface formed at ~ 0.5 ML, we have identified four surface states (S_1 – S_4) with only small dispersions. It is shown that the electronic structure of a 2×2 -Pb surface is very similar to that of a Si(001) 2×2 -Al (In or Ga) surface. This similarity suggests that the surface structure of the 2×2 -Pb surface is proximal to those of the 2×2 surfaces induced by group-III metals. That is, the 2×2 surface is thought to basically consist of the parallel adsorbate-dimer chains on top of the dimerized Si(001) 2×1 surface. The surface states observed on the 2×2 -Pb surface are tentatively assigned following the corresponding surface states of the 2×2 -Al (In) surface: the S_1 surface state to the Pb-Pb dimer-bond state and S_2 and S_3 to the Pb-Si back-bond states of Pb dimers.

On the SD Si(001) 2×1 -Pb surface (the Pb coverage of ~ 1 ML), three distinctive surface-state bands (M , SS_2 , and SS_4) have been observed. Overall, this surface has a significantly different electronic structure from that of the 2×2 -Pb surface at 0.5 ML. Of particular interest is the metallic surface state M located on E_F with almost no dispersion. The ARPES spectra and the LEED patterns of the Pb/Si(001) surface hardly change above 1.0 ML, which indicates that the surface structure does not change drastically during the layer-by-layer growth up to ~ 2 ML's

ACKNOWLEDGMENTS

The authors are grateful to Dr. K. Sakamoto and Dr. T. Sakamoto for providing a well-oriented Si(001) wafer. This work was performed under Photon Factory Proposal No. 97-G307.

*Author to whom correspondence should be addressed. FAX: +82-2-312-709. Electronic address: yeom@phy.yonsei.ac.kr

¹S. Froyen, D. M. Wood, and A. Zunger, Appl. Phys. Lett. **54**, 2435 (1989).

²M. Gell, Appl. Phys. Lett. **55**, 484 (1989).

³D. J. Eaglesham, H.-J. Gossmann, and M. Cerullo, Phys. Rev. Lett. **65**, 1227 (1990).

⁴M. V. R. Murty, H. Atwater, A. J. Kellock, and J. E. E. Baglin, Appl. Phys. Lett. **62**, 2566 (1993).

⁵For example, Ph. Sonnet, L. Stauffer, and C. Minot, Surf. Sci. **407**, 121 (1998); J. M. Gómez-Rodríguez, J. J. Sáenz, A. M. Baró, J.-Y. Veuillen, and R. C. Cinti, Phys. Rev. Lett. **76**, 799 (1996).

⁶H. Itoh, H. Tanabe, D. Winau, A. K. Schmid, and T. Ichinokawa, J. Vac. Sci. Technol. B **12**, 2086 (1994).

⁷L. Li, C. Koziol, K. Wurm, Y. Hong, E. Bauer, and I. S. T. Tsong, Phys. Rev. B **50**, 10 834 (1994).

⁸J.-Y. Veuillen, J.-M. Gómez-Rodríguez, and R. C. Cinti, J. Vac. Sci. Technol. B **14**, 1010 (1996).

⁹J. Nogami, A. A. Baski, and C. F. Quate, Phys. Rev. B **44**, 1415 (1991).

¹⁰H. Itoh, J. Itoh, A. Schmid, and T. Ichinokawa, Phys. Rev. B **48**, 14 663 (1993).

¹¹M. M. R. Evans and J. Nogami, Phys. Rev. B **59**, 7644 (1999), and references therein.

¹²H. Sakama, K. Murakami, K. Nishikata, and A. Kawazu, Phys. Rev. B **48**, 5278 (1993).

¹³Y. Qian, M. J. Bedzyk, S. Tang, A. J. Freeman, and G. E. Franklin, Phys. Rev. Lett. **73**, 1521 (1994).

¹⁴H. W. Yeom, T. Abukawa, Y. Takakuwa, Y. Mori, T. Shimatani, A. Kakizaki, and S. Kono, Phys. Rev. B **53**, 1948 (1996), and references therein.

¹⁵H. W. Yeom, T. Abukawa, Y. Takakuwa, Y. Mori, T. Shimatani, A. Kakizaki, and S. Kono, Phys. Rev. B **54**, 4456 (1996).

¹⁶H. W. Yeom, T. Abukawa, Y. Takakuwa, Y. Mori, T. Shimatani, A. Kakizaki, and S. Kono, Phys. Rev. B **55**, 15 669 (1997).

¹⁷J. C. Glueckstein, M. M. R. Evans, and J. Nogami, Surf. Sci. **415**, 80 (1998).

¹⁸W. S. Yang, X.-D. Wang, K. Cho, J. Kishimoto, T. Hashizume, and T. Sakurai, Phys. Rev. B **51**, 7571 (1995).

¹⁹G. Falkenberg, L. Seehofer, R. Rettig, and R. L. Johnson, Surf. Sci. **372**, 155 (1997).

- ²⁰P. J. Bedrossian, Phys. Rev. Lett. **74**, 3648 (1995).
- ²¹J. van Wingerden, A. van Dam, M. J. Haye, P. M. L. O. Scholte, and F. Tuinstra, Phys. Rev. B **55**, 4723 (1997).
- ²²X. R. Qin and M. G. Lagally, Science **278**, 1444 (1997).
- ²³M. E. Gonzolez-Mendez and N. Takeuchi, Phys. Rev. B **58**, 16 172 (1998).
- ²⁴N. Takeuchi, Surf. Sci. **412/413**, 358 (1998).
- ²⁵H. W. Yeom, T. Abukawa, Y. Takakuwa, M. Nakamura, M. Kimura, A. Kakizaki, and S. Kono, Surf. Sci. **321**, L177 (1994).
- ²⁶H. W. Yeom, T. Abukawa, M. Nakamura, S. Suzuki, S. Sato, K. Sakamoto, T. Sakamoto, and S. Kono, Surf. Sci. **341**, 328 (1995), and references therein.
- ²⁷H. W. Yeom, T. Abukawa, Y. Takakuwa, M. Nakamura, M. Kimura, A. Kakizaki, and S. Kono, Surf. Sci. **365**, 328 (1996).
- ²⁸R. G. Zhao, J. F. Jia, and W. S. Yang, Surf. Sci. Lett. **274**, L519 (1992).
- ²⁹S. Odasso, M. Göthelid, V. Yu. Aristov, and G. Le Lay, Surf. Rev. Lett. **5**, 5 (1998).
- ³⁰H. W. Yeom, I. Matsuda, K. Tono, and T. Ohta, Phys. Rev. B **57**, 3949 (1998).
- ³¹Y. Enta, S. Suzuki, and S. Kono, Surf. Sci. **242**, 277 (1991); H. W. Yeom, T. Abukawa, M. Nakamura, S. Suzuki, S. Sato, K. Sakamoto, and S. Kono, *ibid.* **341**, 328 (1995).
- ³²L. S. O. Johansson, R. I. G. Uhrberg, P. Mårtensson, and G. V. Hansson, Phys. Rev. B **42**, 1305 (1990), and references therein.
- ³³Y. Enta, S. Suzuki, and S. Kono, Phys. Rev. Lett. **65**, 2704 (1990).
- ³⁴Y. Enta, S. Suzuki, and S. Kono, Surf. Sci. **242**, 277 (1991); Y. Enta, Ph.D. thesis, Tohoku University, Japan, 1990.
- ³⁵G. Le Lay, K. Hricovini, and J. E. Bonnet, Phys. Rev. B **39**, 3927 (1989).